Quantum-mechanical Hartree-Fock self-consistent-field study of the elastic constants and chemical bonding of MgF_2 (sellaite)

M. Catti
Department of Physical Chemistry and Electrochemistry, University of Milano, via Golgi 19, I-20133 Milano, Italy

A. Pavese
Department of Earth Sciences, Section of Mineralogy and Crystallography, University of Torino, via V. Caluso 37, I-10125 Torino, Italy

R. Dovesi, C. Roetti, and M. Causà
Department of Inorganic, Physical and Materials Chemistry, University of Torino, via Giuria 5, I-10125 Torino, Italy

(Received 6 March 1991)

A periodic *ab initio* Hartree-Fock method (the program CRYSTAL) has been used to evaluate the total-electron-energy surface of MgF_2 (rutile-type tetragonal structure) as a function of crystal strain. Mg and F atoms are represented by 13 atomic orbitals in the form of contracted Gaussian-type functions. The equilibrium unit-cell edges and fluorine coordinates, the binding energy, and the six elastic constants C_{11}, C_{12}, C_{13}, C_{33}, C_{44}, and C_{66} have been calculated. Inner strain was accounted for by relaxing the F-atom position for each lattice deformation applied, and contributed significantly to the C_{44}, C_{66}, and C_{33} components. An average deviation of 8.0% is observed with respect to experimental elastic data. Classical two-body empirical calculations have been performed for the purpose of comparison. Energy bands, Mulliken electron populations, and charge-density maps are analyzed, and the chemical bonding is discussed, showing significant deviations from ionicity ($z_{Mg}=1.80|e|$).

I. INTRODUCTION

Quantum-mechanical calculations of the elastic properties of ionic crystals have mostly been based on the electron-gas approximation,[1] and have found applications to the alkali-metal and alkaline-earth halides and oxides,[2] also in the "potential-induced-breathing" version.[3–8] Other studies have used elementary tight-binding methods[9] or local-density-functional theory.[10–14] These approaches can be compared with the conventional classical calculations based on semiempirical two-body potentials of the Born type,[15,16] often including the dipole shell model or the breathing shell model.[17–19]

Recently a straightforward *ab initio* Hartree-Fock method has been applied to fluorite CaF_2,[20] using the computer program CRYSTAL.[21,22] The hypersurface of the total electron energy of the crystal is calculated point by point for suitable changes of the unit-cell geometry (lattice strain) and of the atomic fractional coordinates (inner strain). The elastic constants are then computed numerically as second derivatives of the energy with respect to strain components. In view of the encouraging results obtained for cubic CaF_2, this approach has been extended here to the more complex MgF_2 (sellaite), which is tetragonal $P4_2/mnm$ with two formula units in the unit cell.[23] The crystal structure is the same of rutile TiO_2 (Fig. 1), and while the Mg atoms are fixed on symmetry centers, the fluorines have a positional degree of freedom $x(F)=y(F)$. There are six independent components of the elasticity tensor, instead of three as in the cubic case; moreover, owing to the lower symmetry, a more important role is expected to be played in the elastic constants by inner strain.

The rutile-type structure is observed in several metal difluorides and dioxides of interest for their physical and

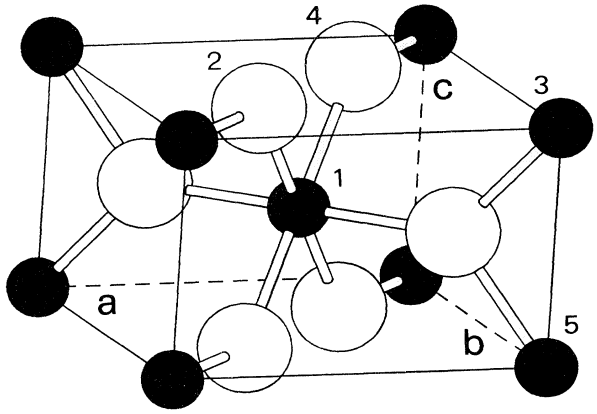

FIG. 1. Tetragonal unit cell of MgF_2 (rutile-type structure). Closed and open circles represent Mg and F atoms, respectively. The atom numbering defines planes of maps in Figs. 5–8.

chemical properties, so that results obtained for MgF_2 can be used to model other members of the family as well. Further particular attention is to be paid to the characterization of electron properties and chemical bonding, because some features of the rutile structure (distortions and linkages of the cation coordination octahedra) would suggest some deviations from pure ionicity.[24] In previous studies, the electron band structure of MgF_2 was explored by a combined tight-binding and pseudopotential method,[25] with the aim of interpreting the optical behavior; the equilibrium properties (structural variables and binding energy) were calculated both by the electron-gas approximation[2] and by empirical classical simulations.[26]

II. METHOD OF CALCULATION

The all-electron *ab initio* self-consistent-field (SCF) Hartree-Fock linear combination of atomic orbitals (HF LCAO) computational scheme, as implemented in CRYSTAL (Ref. 22) was described in previous papers.[21] CRYSTAL is a general program for the treatment of crystalline compounds of any space group, which was applied to the study of semiconductors and molecular crystals, slabs, and polymers. As regards ionic crystals, LiH,[27] Li_2O,[28] Li_3N,[29] and MgO (Ref. 30) were studied. Recent improvements in the accuracy and speed of the program allow one now to evaluate elastic constants by computing the numerical second derivatives of the energy.[20]

The basis set adopted for the present calculations is reported in Table I. Thirteen "atomic orbitals" have been used for magnesium and fluorine. Each atomic orbital is a linear combination ("contraction") of Gaussian-type functions (GTF), which are the product of a radial Gaussian times a real solid harmonic function. In the notation of Ref. 31, the two basis sets are indicated as 8-511G and 7-311G, respectively, where the numbers refer to the level of contraction. The exponents and coefficients of the inner shells were fully optimized in parallel studies devoted to MgO and LiF; the exponents of valence shells were optimized in the present study. The effect of *d* functions on the investigated properties has been shown to be negligible. On the whole, the present basis set appears adequate to provide a high quality description of the ground-state properties of MgF_2.

A possible source of error in the present study is due to the intrinsic limits on the Hartree-Fock approximation ("correlation error"). It is well known[31] from molecular experience that the Hartree-Fock approach underestimates (in covalent systems) the binding energies by about 30%, whereas the bond lengths are overestimated by 0.5–1 %. Similar results were obtained in a systematic study devoted to IV-IV and III-V semiconductors.[32] As regards ionics, the few previous studies seem to confirm this trend, although more experience is required both in terms of explored properties and type of ions considered. As will be shown in the following, the HF binding energy can easily be corrected in order to take into account the correlation contribution.

III. EQUILIBRIUM STRUCTURE AND BINDING ENERGY

The unit-cell edges *a* and *c* and the fluorine fractional coordinate *x*(F) determined at 52 K by neutron

TABLE I. Exponents ($bohr^{-2}$) and coefficients of the Gaussian functions adopted for the present study. The contraction coefficients multiply individually normalized Gaussian. $y[\pm z]$ stands for $y \times 10^{\pm z}$.

Shell	Fluorine			Magnesium		
		Coefficients			Coefficients	
type	Exponents	*s*	*p*	Exponents	*s*	*p*
1*s*	1.377[+4]	8.770[−4]		6.837[+4]	2.226[−4]	
	1.590[+3]	9.150[−3]		9.699[+3]	1.898[−3]	
	3.265[+2]	4.860[−2]		2.041[+3]	1.105[−2]	
	9.166[+1]	1.691[−1]		5.299[+2]	5.006[−2]	
	3.046[+1]	3.708[−1]		1.592[+2]	1.691[−1]	
	1.150[+1]	4.165[−1]		5.469[+1]	3.670[−1]	
	4.76	1.306[−1]		2.124[+1]	4.004[−1]	
				8.746	1.499[−1]	
2*sp*	1.9[+1]	−1.094[−1]	1.244[−1]	1.568[+2]	−6.24[−3]	7.22[−3]
	4.53	−1.289[−1]	5.323[−1]	3.103[+1]	−7.882[−2]	6.427[−2]
	1.37	1.0	1.0	9.645	−7.992[−2]	2.104[−1]
				3.711	2.906[−1]	3.431[−1]
				1.612	5.716[−1]	3.735[−1]
3*sp*	4.5[−1]	1.0	1.0	6.8[−1]	1.0	1.0
4*sp*	2.05[−1]	1.0	1.0	2.8[−1]	1.0	1.0

TABLE II. Minimum-energy and experimental values of unit-cell edges (Å) and volume (Å^3) of MgF_2; x(F) is the fractional coordinate of fluorine. Δ (%) is the percentage error.

	Calculated	Experimental (Ref. 23)	Δ (%)
a	4.637	4.615	+0.5
c	3.087	3.043	+1.4
V	66.4	64.8	+2.5
x(F)	0.3032	0.3030	+0.1

diffraction[23] are considered to be a good approximation to the 0 K experimental crystal structure of MgF_2, and are reported in Table II. The calculated equilibrium structural configuration has been obtained by minimizing the total crystal energy with respect to a, c, and x(F). Steps of 0.06 Å, 0.05 Å, and 0.005 were considered for the three variables, respectively. At first the cell edges only were changed, keeping x(F) fixed at its experimental value; then x(F) was varied separately. Polynomial interpolations yielded the minimum-energy results (Table II). These show quite good agreement with measured data, within the well-known tendency of HF calculations to overestimate unit-cell volumes;[32] for instance, in the case of CaF_2,[20] the relative error for volume was +5.2%. A larger deviation for c than for a is observed, indicating that the minimum-energy cell is slightly more elongated along the fourfold axis than the experimental one (c/a=0.6657 against 0.6594). On the other hand, the change of fluorine coordinate is hardly significant.

By applying a conventional Born-Haber thermochemical cycle to the formation process of MgF_2 from solid Mg and gaseous F_2 at 298 K, the experimental value of the binding energy has been obtained (Table III). Appropriate values of formation enthalpy ΔH_f of MgF_2, cooling energies of Mg and F_2 down to 0 K, and energies of sublimation of Mg and dissociation of F_2 molecules have been used.[33] The zero-point vibrational energy, evaluated by the Debye model (Θ_D=597 K, from Ref. 34), was subtracted.

The total crystal energy has been computed for the minimum-energy structural parameters (Table II) and the optimized basis set (Table I). The total energy of isolated atoms was evaluated starting from the crystalline basis. In the case of fluorine the exponents of the two most diffuse Gaussians were reoptimized (α=0.44 and 0.15 bohr^{-2}). For magnesium the basis set of Table I, essentially designed to describe an ionic situation, was supplemented by two diffuse sp shells, in order to provide additional variational freedom accounting for the tails of the atomic wave function. By optimizing the exponents of the two shells, the values 0.073 and 0.023 bohr^{-2} were obtained. The difference between crystal and atomic HF energies is BE (HF), the Hartree-Fock approximation to the binding energy, which is about 20% smaller than the experimental value (Table III).

The electron correlation contribution to BE was estimated in two ways, the resulting values being indicated as δE_1 and δE_2 in Table II. δE_1 is the difference of correlation energy between the pairs Mg-Mg^{2+} and F-F^-, the data for isolated atoms and ions being taken from Ref. 35. In this model all the correlation contribution to BE is ascribed to charge transfer, whereas the contribution from relaxation of the atomic and ionic wave functions due to the crystalline field is disregarded. Table II shows that this correction accounts for about 90% of the difference between the experimental and the HF BE, confirming that polarization effects and other mechanisms play a minor role in the present case. δE_2 is the difference between the correlation energy of the crystal and of the atoms, evaluated with the density-functional formula proposed in Ref. 36 and applied to the HF charge density. In this case the correction accounts for about 75% of the difference between the HF and the experimental BE.

TABLE III. HF total energy at equilibrium (per MgF_2 unit formula), atomic energies, and binding energy (BE) (hartree). δE_1 is the correlation contributions to BE evaluated from the correlation energy difference between the isolated atoms and ions; δE_2 is the contribution to BE calculated by using the charge-density functional of Ref. 36. Δ (%) is the percentage error with respect to BE (expt.). DF stands for density functional.

	MgF_2	Mg	F
E (HF)	−398.775 533	−199.597 427	−99.374 016
BE (HF)	−0.430		
Δ (%)	+20.5		
	Correlation contributions		
δE_1 (ion. corr.)	−0.106	0.042	−0.074
BE (HF ion. corr.)	−0.536		
Δ (%)	+2.1		
Correlation energy	−1.202	−0.466	−0.324
δE_2 (DF corr.)	−0.088		
BE (HF+DF corr.)	−0.518		
Δ (%)	+5.4		
BE (expt.)	−0.548[a]		

[a]Born-Haber cycle from thermochemical data (Ref. 33).

IV. ELASTIC PROPERTIES

Data calculated by the present method ignore all vibrational contributions to the energy, and thus should be compared to experimental values at 0 K corrected for the effect of zero-point vibrations. By plotting elastic constants against temperature a linear increase is generally observed as T decreases down to about 200 K: at lower temperatures the increase is less than linear, so that extrapolation to 0 K is required to omit the zero-point contribution.[37,38,20] The elastic constants of MgF_2 were measured in the 4.2–300 K (Ref. 34) and 300–500 K (Ref. 39) ranges by ultrasonic techniques. Linear extrapolations to absolute zero give very similar results in both cases for all elastic components but C_{13} and C_{66}, which do not show a range of linearity in the low-temperature

TABLE IV. Calculated and experimental elastic constants (GPa) of MgF_2. External elastic constants are evaluated without reoptimizing the fractional coordinate of fluorine x(F); inner values are corrections for atomic relaxation. Δ (%) is the percentage error with respect to the experimental value. C_{12} and C_{13} are derived from the reported linear combinations. The error due to numerical evaluation of the energy second derivative is within 1 GPa.

	Calculated				
	External	Inner	Total	Experimental[a]	Δ (%)
C_{11}	156.3	−1.0	155.3	145.6	+6.7
C_{12}	91.8	−1.1	90.7	95.2	−4.7
C_{13}	56.6	−1.0	55.6	67.0	−17.0
C_{33}	228.1	−8.8	219.3	214.2	+2.4
C_{44}	78.0	−9.8	68.2	58.3	+17.0
C_{66}	108.1	−4.0	104.1	103.8	+0.3
$C_{11}+C_{12}$	247.9	−1.9	246.0	240.8	+2.2
$C_{11}+C_{12}+2C_{13}+C_{33}/2$	474.5	−9.3	465.2	481.9	−3.5
B	105.0	−1.7	103.3	106.2	−2.7

[a]Extrapolated at 0 K using data from Ref. 39.

data; then the results of Ref. 39 have been preferred and are reported in Table IV. The bulk modulus B has been derived from C_{ij} values by the appropriate formulas.

Elastic constants have been evaluated as second derivatives of the total crystal energy with respect to strain components η_i, according to a second-order expansion of the elastic energy of type

$$E=\tfrac{1}{2}\sum_{i,j=1}^{6} C_{ij}\eta_i\eta_j \ ; \tag{1}$$

the Voigt contraction of subscripts for tensorial components is understood. Suitable lattice deformations $\boldsymbol{\eta}=[\eta_1\,\eta_2\,\eta_3\,\eta_4\,\eta_5\,\eta_6]$ with equal nonzero components were considered, in order to express E as a parabolic function of a single η parameter, whose coefficient represents a linear combination of elastic constants C_{ij}. Each diagonal constant C_{ii} was computed straightforwardly with only η_i as nonzero strain component ($\eta_j=0$ for $j\neq i$), while for the off-diagonal terms C_{12} and C_{13} the $[\eta\,\eta\,0\,0\,0]$ and $[\eta\,\eta\,\eta\,0\,0\,0]$ deformations were applied. These do not break the tetragonal symmetry of the unit cell, unlike those used for computing the C_{11}, C_{44}, and C_{66} constants, and when substituted into (1) they lead to the $C_{11}+C_{12}$ and $C_{11}+C_{12}+2C_{13}+C_{33}/2$ linear combinations, respectively. A larger numerical error affects C_{12} and C_{13}, with respect to the other constants, because they are derived indirectly from linear combinations. Six to eight values of η were used in each case, corresponding to changes of cell edges and angles in the ranges ±0.10 Å and ±5.5°, respectively. The computed energies E were least-squares fitted to polynomial functions of η up to the fourth order, yielding the searched $d^2E/d\eta^2$ derivatives.

An important point to take into account is the possible positional relaxation of fluorine atoms in the unit cell (inner deformation) caused by lattice strain. If that effect is neglected by keeping the atomic fractional coordinates constant, then an upper limit (external component) is obtained for the value of each elastic constant;[40] the results of our calculation for this case are reported in the first column of Table IV. Now let the F atom be displaced by a vector $\mathbf{u}$ from the position corresponding to a pure lattice deformation: then the energy $E_0(\boldsymbol{\eta})$ of the unrelaxed configuration decreases according to $E(\mathbf{u},\boldsymbol{\eta})=E_0(\boldsymbol{\eta})+E_r(\mathbf{u},\boldsymbol{\eta})$, where the latter term is the negative relaxation energy. By requiring E to be a minimum with respect to $\mathbf{u}$ the equation $(\nabla E_r)_{\mathbf{u}}=0$ is obtained, which can be solved for the inner strain $\mathbf{u}(\boldsymbol{\eta})$; by substitution the energies $E_r(\boldsymbol{\eta})$ and $E(\boldsymbol{\eta})$ turn out to be functions of $\boldsymbol{\eta}$ only. The quantities $\partial^2E_0/\partial\eta_i\partial\eta_j$ and $\partial^2E_r/\partial\eta_i\partial\eta_j$ are the external and internal components, respectively, of the elastic constant $C_{ij}=\partial^2E/\partial\eta_i\partial\eta_j$. This procedure is normally applied in two-body classical models in an analytical form, by assuming a bilinear dependence of E on $\boldsymbol{\eta}$ and $\mathbf{u}$ components.[41]

In quantum calculations only a numerical approach is presently feasible; this was used, on the basis of polynomial interpolations, for evaluating the C_{44} elastic constant of fluorite.[20] The case of MgF_2 is more complex, however, because of the tetragonal rather than cubic symmetry: then for each lattice strain $\boldsymbol{\eta}$ considered the symmetry constraints on the displacement vector $\mathbf{u}$ of F have to be determined. For the C_{33}, C_{12}, and C_{13} elastic constants the $\boldsymbol{\eta}$ deformations used do not break the tetragonal symmetry, so as to keep the two conditions $u_x=u_y$ and $u_z=0$. On the other hand, the first constraint is removed in the less symmetrical lattice strains appropriate for the C_{11} and C_{66} constants, and the second one as well in the lowest symmetry case of C_{44}. For simplicity, however, in all calculations the condition $u_x=u_y$ was kept, so that a single u_x component remained except for the C_{44} case where a second component u_z was added. To reduce the computing time, the relaxation en-

ergy $E_r(u_x,u_z,\eta)$ was minimized with respect to u_x (or to u_x and u_z) for the two end values of the η range only, and then a parabolic interpolation yielded the $E_r(\eta)$ curve for all η values. By similar interpolations also the functions $u_x(\eta)$ and $u_z(\eta)$ were obtained. In the case of C_{44}, the two-dimensional minimization was performed with respect to the u_x and u_z variables separately; the relaxation energy turns out to be $E_r(\eta)=-0.060\,146\eta^2$ hartrees. The geometrical effects of the inner deformation on the coordination octahedron of Mg can be appreciated by defining a distortion index as root-mean-square relative deviation of the six individual Mg-F distances from their average value (0.5% in the equilibrium structure). Pure lattice strains usually change that index significantly, while relaxing the fluorine positions tends to bring back the octahedron distortion close to its equilibrium value. For instance, a change of 5.5° of the α angle turns the distortion index into 2.6%, which is reduced to 1.8% if F is allowed to relax.

In the second column of Table IV the inner contributions to elastic constants are reported, together with the total calculated values. The relaxation effect appears to be small for the C_{11}, C_{12}, and C_{13} components, but it gives a substantial contribution to C_{33} and C_{66} (4%) and particularly to C_{44} (13%). In the last case most of the effect (10%) is due to the u_z displacement of fluorine. An outstandingly good agreement between calculated and experimental elastic constants is observed for C_{11}, C_{12}, C_{33}, and C_{66}, while the deviation is larger for C_{13} and C_{44}. This confirms the results obtained for CaF_2,[20] where Δ was -0.5%, -4.7%, and $+17.3\%$ for C_{11}, C_{12}, and C_{44}, respectively: the shear constant C_{44} seems to be particularly critical to be reproduced, either because its large inner component needs a more accurate numerical evaluation, or because of more fundamental weaknesses of the Hartree-Fock approximation. In this respect it should be remembered that larger values of elastic constants are to be expected on the basis of HF model features, which overestimate bond lengths and stiffnesses.[31] On the other hand, the deviation of the C_{13} component is due in part to the sum of errors in the linear combination from which it is derived. The sign of the Cauchy deviation is reproduced correctly for C_{12}-C_{66} but is wrong for C_{13}-C_{44}, because these two constants are affected by significant opposite errors. A similar failure occurred in the case of C_{12}-C_{44} of fluorite.[23]

For purpose of comparison, a semiempirical classical computation of the elastic constants and equilibrium structure of MgF_2 was also carried out. The two-body Born-Mayer potential used, $E_{ij}=e^2z_iz_j/r_{ij}+b_{ij}\exp(-r_{ij}/\rho)-d_{ij}/r_{ij}^6$, includes electrostatic, repulsive, and dispersive terms. The dispersive coefficients were calculated by London's formula[42] using polarizability values of 0.094 and 0.853 Å^3 for Mg^{2+} and F^-, respectively; the former is Pauling's free ion polarizability, while the latter was obtained from the refraction index of MgF_2 (Ref. 33) and the Clausius-Mossotti relation. The repulsive coefficients are written as $b_{ij}=\exp[(r_i+r_j)/\rho]$, while the electroneutrality condition gives $2z_F+z_{Mg}=0$. Thus four independent energy parameters r_F, r_{Mg}, ρ, and z_F are required for the computation. These were fitted so as to reproduce the six experimental elastic constants and three structural variables by a least-squares procedure and a set of computer programs based on the analytical calculation of second derivatives of the crystal energy with respect to lattice constants and atomic coordinates.[40,41]

The optimized parameters and the computed values of

TABLE V. Optimized parameters of the Born-type potential used in classical two-body modeling of MgF_2, and calculated values of structural and elastic properties (cf. Tables II and IV for explanations of symbols and units).

	b_{ij} (eV)	d_{ij} (eV Å^6)
F-F	17 039.097	15.168
F-Mg	4 166.274	2.901
Mg-Mg	905.517	0.5557
$z_F=-0.83\|e\|$	$z_{Mg}=+1.66\|e\|$	$\rho=0.215$ Å

	Calculated	Experimental	Δ (%)
a	4.587	4.615	−0.6
c	3.060	3.043	+0.6
V	64.4	64.8	−0.6
x(F)	0.3027	0.3032	−0.2

	External	Inner	Total	Experimental	Δ (%)
C_{11}	149.5	−2.9	146.6	145.6	+0.7
C_{12}	100.4	−0.2	100.2	95.2	+5.3
C_{13}	66.9	−3.8	63.1	67.0	−5.8
C_{33}	223.6	−9.3	214.3	214.2	+0.1
C_{44}	66.9	−9.2	57.7	58.3	−1.1
C_{66}	100.4	−0.5	100.0	103.8	−3.7
B	109.3	−3.1	106.2	106.2	0.0

elastic constants and structural variables are reported in Table V. It should be remarked that an attempt to fix the charges z_i to ideal ionic values gave a definitely worse fit; the best values obtained show a significant discrepancy from a pure ionic model. An average deviation of 2.8% from experimental values is observed for the elastic data, to be compared with 8.0% of the quantum HF-SCF results. These are then confirmed to be satisfactory, as obtained by first-principles calculations free from empirical parametrization. Also the inner contributions to elastic constants of the classical model (Table V) are in a semiquantitative agreement with those of Table IV, indicating a consistent physical basis for the partition of the elastic response into lattice and inner effects. As for the Cauchy deviations, the sign is reproduced correctly for C_{13}-C_{44} but not for C_{12}-C_{66}, contrary to Hartree-Fock results.

V. ENERGY BANDS AND CHARGE DENSITY

The energy bands were computed along the lines Γ-Z and Γ-X in the first Brillouin zone. In Fig. 2 an overview of the two upper sets of filled bands and of the lowest empty conduction bands is shown. The typical features of ionic crystals, small dispersion and large gaps, appear clearly: the gap width between valence and conduction bands at the Γ point is about 20 eV, against an experimental value of 12.4 eV from reflectance measurements.[43] The Hartree-Fock approximation is well known to overestimate energy gaps, and this effect is increased here

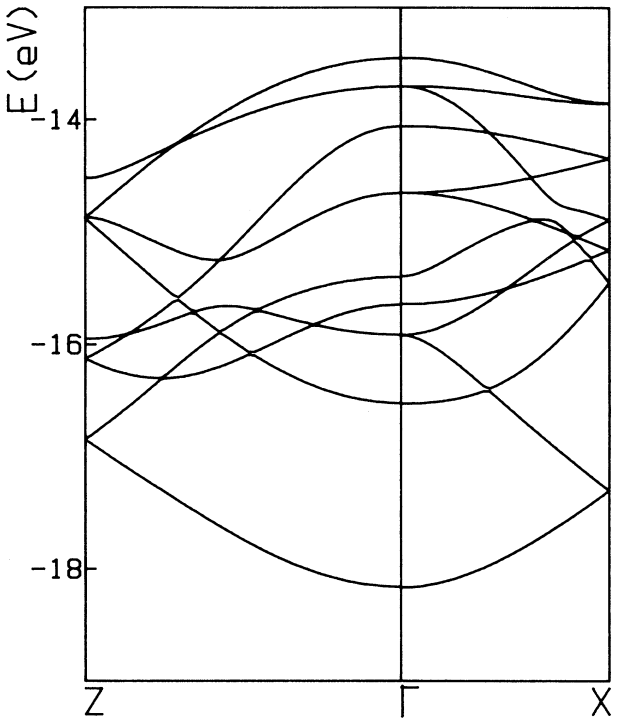

FIG. 3. Details of the set of valence bands showing degenerate branches along the fourfold symmetry direction Γ-Z.

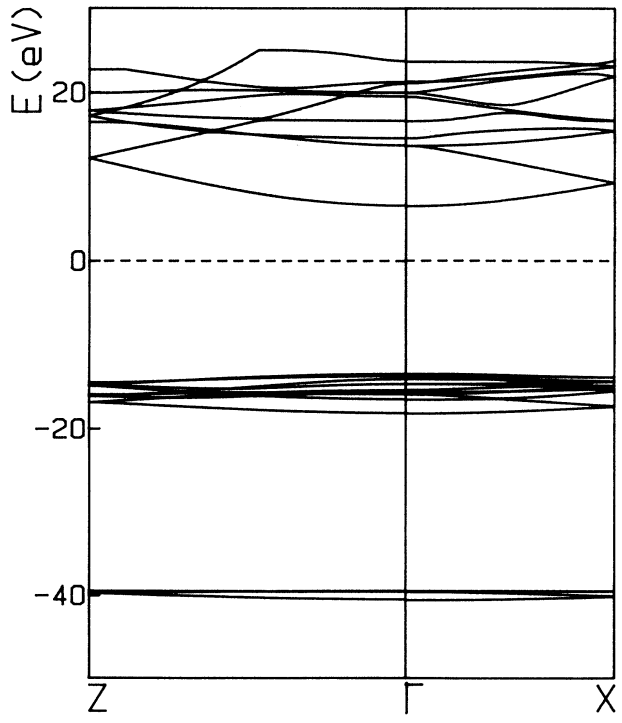

FIG. 2. Electron energy bands of MgF_2 along two symmetry lines in the first Brillouin zone.

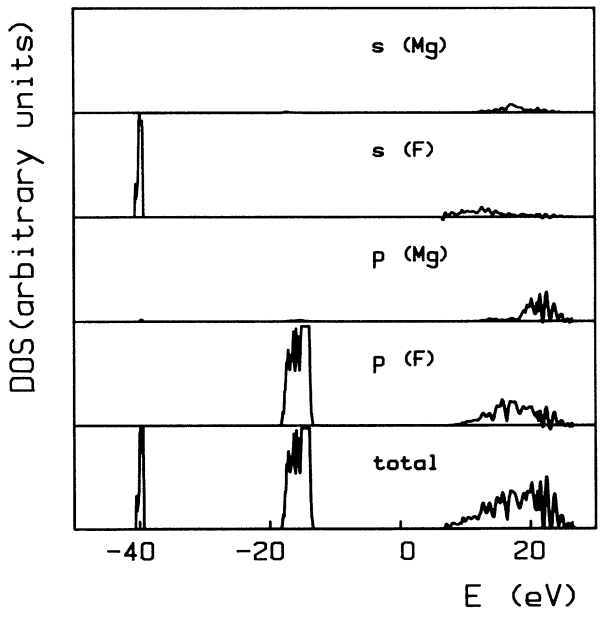

FIG. 4. Projected and total densities of states (DOS) of MgF_2. A Mulliken partition scheme was used to obtain atomic orbital contributions.

because the basis set, though adequate for representing the ground state, lacks diffuse valence orbitals on Mg and is then unsatisfactory for excited states. A previous calculation[25] of the band structure of MgF_2 used a tight-binding method for the valence bands and a pseudopotential model for the conduction states, considering an extra electron added to the lattice and seeing the potential of closed-shell ions. Though this method was claimed to be suitable for reproducing optical properties, it gave a theoretical gap of 20.5 eV, which had then to be corrected by polarization energy terms in order to obtain a calculated optical gap of 12.8 eV. The set of valence bands is shown in detail in Fig. 3, displaying clearly the degeneracy of several branches along the high symmetry direction Γ-Z, which is removed along Γ-X.

A better insight into chemical bonding is obtained by inspection of the total and projected densities of electronic states (Fig. 4). The two upper filled bands correspond to nearly pure s and p states of fluorine, respectively; it is interesting to remark that occupied bands related to Mg closed shells are deeper in energy, while in the CaF_2 case[20] a p(Ca) band lies between the s(F) and p(F) states. The main contribution to the conduction band is given by p-type outer orbitals on both F and Mg, and by s-type to a minor extent.

The degree of ionicity of chemical bonding in MgF_2 can be estimated by results of a Mulliken population analysis. Net charges of $+1.803|e|$ on Mg and $-0.901|e|$ on F are obtained, which deviate significantly from ideal ionic values. The Mg charge can be compared with that

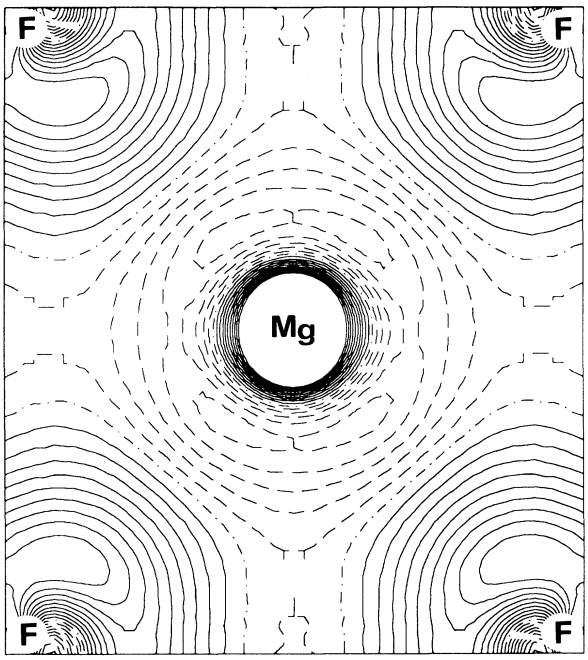

FIG. 6. Difference (crystal minus ionic superposition) electron density map on the $(1\bar{1}0)$ plane. Continuous, dot-dashed, and dashed lines indicate positive, zero, and negative values, respectively. Isodensity curves are separated by $0.001e/(\text{bohr})^3$.

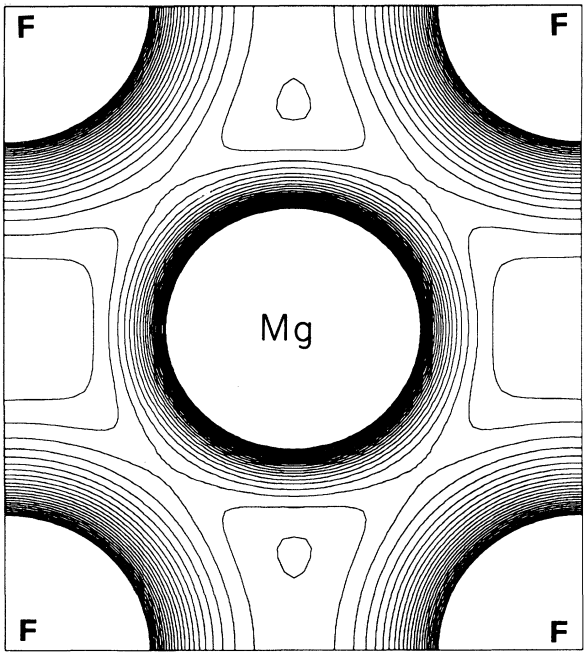

FIG. 5. Total electron density map on the $(1\bar{1}0)$ plane through Mg and F atoms (1-2-4 in Fig. 1). Isodensity curves are separated by $0.01e/(\text{bohr})^3$.

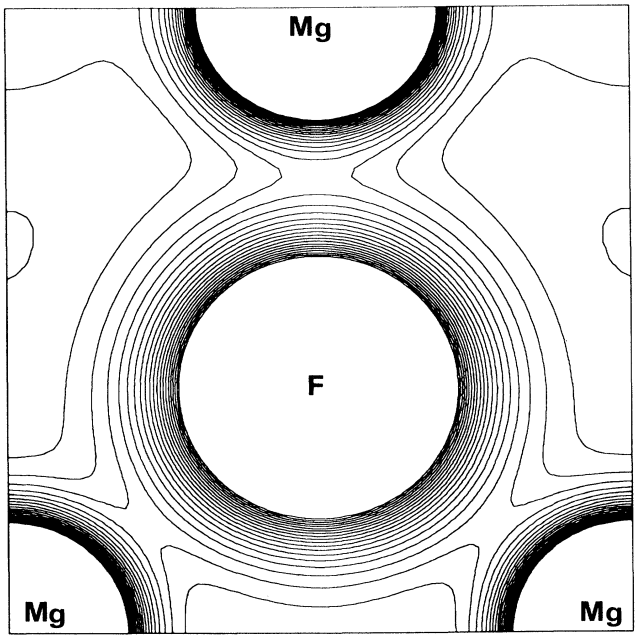

FIG. 7. Total electron density map on the (110) plane through Mg and F atoms (1-3-5 in Fig. 1). Isodensity curves are separated by $0.01e/(\text{bohr})^3$.

on Ca in fluorite, $+1.868|e|$, and shows a consistent increasing trend with the mass of the alkaline-earth cation. Also the comparison with charge values obtained from the two-body semiempirical model (Table V) is not unreasonable, considering that the inclusion of a dispersion term (which is not taken into account in the Hartree-Fock calculation) lowers the electrostatic part of the attractive energy and then decreases the atomic charges. The bond population analysis gives an average positive value of $0.018e$/bohr^3 for the two independent Mg-F bonds, indicating a slight covalent component which is consistent with the values of atomic charges. These results contrast somehow with the Mulliken charge of $1.950|e|$ on Mg obtained in a previous study[30] of MgO, which indicated a fully ionic behavior. Taking into account that in all cases the same computing method and program were used, the different behavior observed for Mg and Ca fluorides and for Mg oxide seems to be significant. This might be related to the rocksalt structure of MgO being more suitable for full ionic bonding than the rutile or fluorite structures, partly because in the latter cases the anions show much lower coordination numbers (three and four, respectively, against six in MgO).

The electron charge density has been computed on planes $(1\bar{1}0)$ and (110) in the structure of MgF_2 (cf. Fig. 1), emphasizing the coordination environments of Mg^{2+} and F^- ions, respectively. Total and difference maps are shown in Figs. 5 and 6 and in Figs. 7 and 8 for the two planes; the difference is meant between total crystal and ionic superposition densities. In both cases the electron clouds of anions and cations appear to contract substantially in the crystal with respect to the free ion state. This effect should be ascribed mainly to electron exchange repulsion, according to Pauli's exclusion principle, but also to compression produced by the crystal electrostatic field on the electron cloud. However, the density contraction appears much larger for Mg^{2+} than for F^-, in contrast with the behavior of fluorite where this effect was quite comparable for anion and cations. It should be remarked that the contraction of both the anion and cation as a result of crystal formation agrees with results of the breathing shell model,[17,18] but disagrees with the potential-induced-breathing model,[3–8] according to which the cation should expand instead of contract by effect of the crystal Coulomb field.

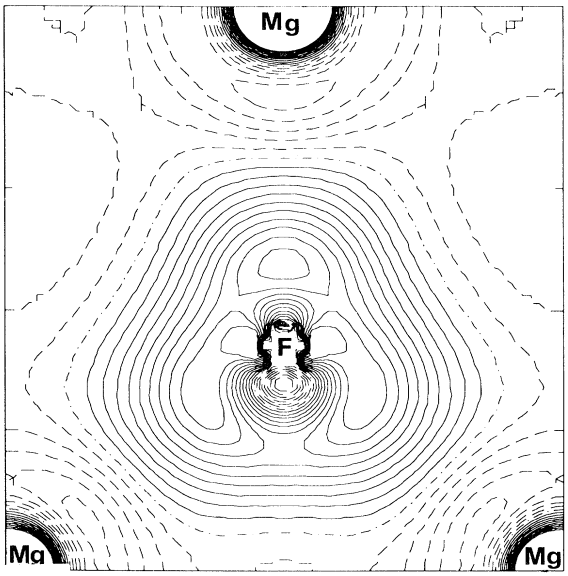

FIG. 8. Difference electron density map on the (110) plane. Isodensity curves are separated by $0.001e$/(bohr)^3.

VI. CONCLUSIONS

The quantum-mechanical evaluation of elastic constants by *ab initio* Hartree-Fock methods has been extended to a noncubic crystal, MgF_2, with a fairly complex structure for this approach. A satisfactory overall agreement with experimental data is observed. Positive and negative errors are obtained for shear diagonal and for extra-diagonal components of the elastic tensor, respectively, confirming the results of a similar study on cubic CaF_2. Opposite sources of error are neglecting the electron correlation energy in the HF model,[31] which makes the crystal stiffer and increases the elastic constants, and using the larger calculated unit-cell volume, which lowers the crystal rigidity. On the other hand, it is not fully clear why just the extra-diagonal components are systematically underestimated: possible deficiencies of the atomic basis set might play a role in this respect. The inner-strain effect has been investigated deeply, proving to give important contributions to crystal elasticity, consistent with the results of classical Born-type simulations. Evidence for a significant deviation from ideal ionic bonding in MgF_2 is obtained by a Mulliken population analysis, again in substantial agreement with two-body semiempirical models.

ACKNOWLEDGMENTS

Financial support by the Ministero Università e Ricerca Scientifica e Tecnologica (Roma) and by Consorzio per il Sistema Informativo Piemonte (Torino) is gratefully acknowledged.

[1]R. G. Gordon and Y. S. Kim, J. Chem. Phys. **56**, 3122 (1972).
[2]C. Muhlhausen and R. Gordon, Phys. Rev. B **23**, 900 (1981).
[3]C. Muhlhausen and R. Gordon, Phys. Rev. B **24**, 2147 (1981).
[4]R. J. Hemley, M. D. Jackson, and R. G. Gordon, Geophys. Res. Lett. **12**, 247 (1985).
[5]M. J. Mehl, R. J. Hemley, and L. L. Boyer, Phys. Rev. B **33**, 8685 (1986).
[6]R. E. Cohen, L. L. Boyer, and M. J. Mehl, Phys. Rev. B **35**, 5749 (1987).
[7]A. P. Jephcoat, R. J. Hemley, H. K. Mao, R. E. Cohen, and M. J. Mehl, Phys. Rev. B **37**, 4727 (1988).
[8]J. L. Feldman, M. J. Mehl, L. L. Boyer, and N. C. Chen, Phys. Rev. B **37**, 4784 (1988).
[9]G. K. Straub and W. A. Harrison, Phys. Rev. B **39**, 10 325

(1989).
[10]J. S. Melvin and D. C. Hendry, J. Phys. C **15**, 2093 (1982).
[11]K. S. Chang and M. L. Cohen, Phys. Rev. B **30**, 4774 (1984).
[12]N. E. Christensen, Phys. Rev. B **33**, 5096 (1986).
[13]M. J. Mehl, R. E. Cohen, and H. Krakauer, J. Geophys. Res. **93**, 8009 (1988).
[14]J. Chen, L. L. Boyer, H. Krakauer, and M. J. Mehl, Phys. Rev. B **37**, 3295 (1988).
[15]C. R. A. Catlow and W. C. Mackrodt, *Computer Simulations of Solids,* Vol. 166 of *Lecture Notes in Physics* (Springer-Verlag, Berlin, 1982).
[16]M. Catti, J. Phys. Chem. Solids **43**, 1111 (1982).
[17]A. D. B. Woods, W. Cochran, and B. N. Brockhouse, Phys. Rev. **119**, 980 (1960).
[18]V. Nusslein and U. Schröder, Phys. Status Solidi **21**, 309 (1967).
[19]A. N. Basu and S. Sengupta, Phys. Status Solidi **29**, 367 (1968).
[20]M. Catti, R. Dovesi, A. Pavese, and V. Saunders, J. Phys. Condens. Matter **3**, 4151 (1991).
[21]C. Pisani, R. Dovesi, and C. Roetti, *Hartree-Fock Ab Initio Treatment of Crystalline Solids,* Vol. 48 of *Lecture Notes in Chemistry* (Springer-Verlag, Berlin, 1988).
[22]R. Dovesi, C. Pisani, C. Roetti, M. Causà, and V. R. Saunders, CRYSTAL88. Program *n*.577, Quantum Chemistry Program Exchange, Indiana University, Bloomington, IN, 1989.
[23]G. Vidal-Valat, J. P. Vidal, C. M. E. Zeyen, and K. Kurki-Suonio, Acta Crystallogr. Sect. B **35**, 1584 (1979).
[24]W. H. Baur, 1976, Acta Crystallogr. Sect. B **32**, 2200 (1976).
[25]C. Jouanin, J. P. Albert, and C. Gout, J. Phys. (Paris) **37**, 595 (1976).
[26]P. S. Yuen, R. M. Murfitt, and R. L. Collin, J. Chem. Phys. **61**, 2383 (1974).
[27]R. Dovesi, C. Ermondi, E. Ferrero, C. Pisani, and C. Roetti, Phys. Rev. B **29**, 3591 (1984).
[28]R. Dovesi, Int. J. Quantum Chem. **26**, 197 (1984).
[29]R. Dovesi, C. Pisani, F. Ricca, C. Roetti, and V. R. Saunders, Phys. Rev. B **30**, 972 (1984).
[30]M. Causà, R. Dovesi, C. Pisani, and C. Roetti, Phys. Rev. B **33**, 1308 (1986).
[31]W. H. Here, L. Radom, P. R. Schleyer, and J. A. Pople, *Ab Initio Molecular Orbital Theory* (Wiley, New York, 1986).
[32]R. Orlando, R. Dovesi, C. Roetti, and V. R. Saunders, J. Phys. Condens. Matter **2**, 7769 (1990).
[33]*Handbook of Chemistry and Physics,* edited by R. C. Weast (Chemical Rubber Company, Boca Raton, FL, 1987).
[34]H. M. Kandill, J. D. Greiner, A. C. Ayers, and J. F. Smith, J. Appl. Phys. **52**, 759 (1981).
[35]E. Clementi, J. Chem. Phys. **38**, 2248 (1963).
[36]J. P. Perdew, Phys. Rev. B **33**, 8822 (1986).
[37]G. Liebfried and W. Ludwig, Solid State Phys. **12**, 275 (1961).
[38]J. A. Garber and A. V. Granato, Phys. Rev. B **11**, 3990 (1975).
[39]L. E. A. Jones, Phys. Chem. Minerals **1**, 179 (1977).
[40]M. Catti, Acta Crystallogr. Sect. A **41**, 494 (1985).
[41]M. Catti, Acta Crystallogr. Sect. A **45**, 20 (1989).
[42]I. M. Boswarva, Phys. Rev. B **1**, 1698 (1970).
[43]J. Thomas, G. Stephan, J. C. Lemonier, M. Nisar, and S. Robin, Phys. Status Solidi B **56**, 163 (1973).